Recent Results and Perspectives on Multi-Phase Multi-Component Porous Media Flows in Chemical EOR

Prabir Daripa

Department of Mathematics, Texas A&M University
http://www.math.tamu.edu/~daripa

SIAM Geosciences Meeting 2019
Houston, March 11 – 14, 2019
Collaborators: Sourav Dutta and Craig Gin

Introduction

Some of the objectives in EOR (Enhanced Oil Recovery)

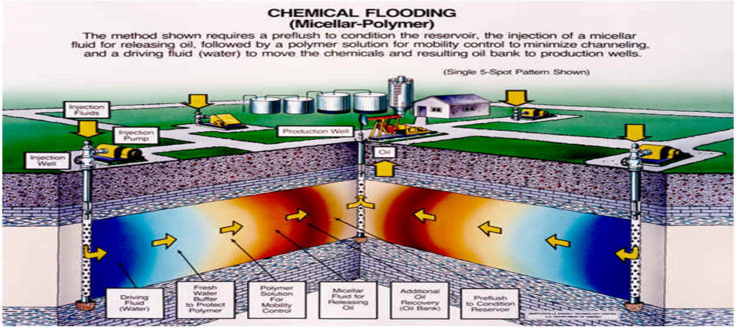

(a) Courtesy of DOE.

To improve oil recovery, EOR processes are designed to control, among many other things, the following:

- Capillary pressure
- Viscous fingering

Role of Polymer and Surfactant

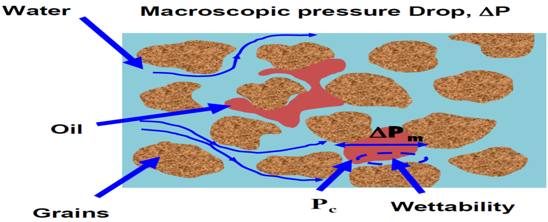

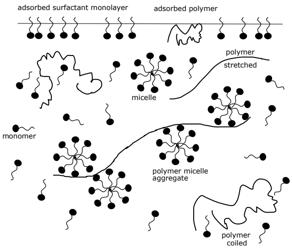

Polymer-surfactant solution

Surfactant

- Reduces capillary forces and residual saturation

Polymer

- Mobility control

Viscous Fingering

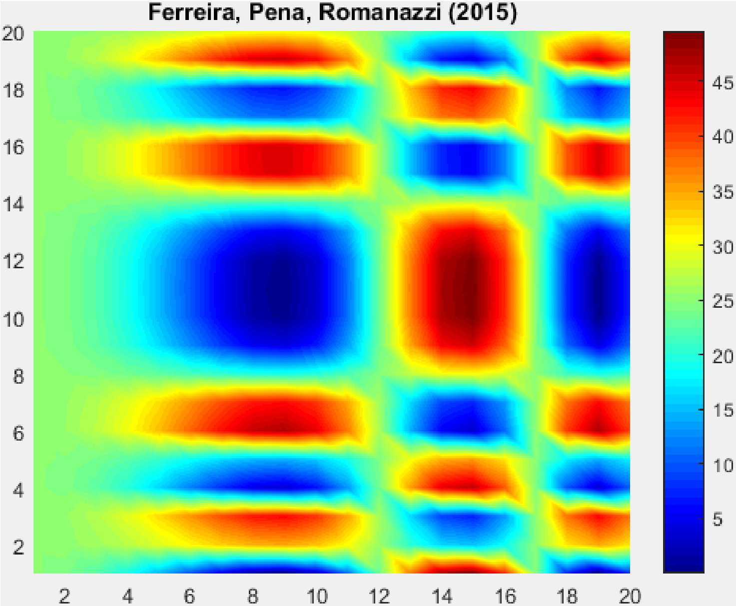

Outcome from this talk

- Viscous fingering in Single- versus Multi-layer interfacial instability in the linear regime: its relevance for chemical EOR.

Outcome from this talk

- Viscous fingering in Single- versus Multi-layer interfacial instability in the linear regime: its relevance for chemical EOR.
- Modeling of chemical EOR by Surfactant-Polymer (SP) Flooding.
- A new hybrid method for solving SP flooding problems, its salient features, and some numerical results.

Outcome from this talk

- Viscous fingering in Single- versus Multi-layer interfacial instability in the linear regime: its relevance for chemical EOR.
- Modeling of chemical EOR by Surfactant-Polymer (SP) Flooding.
- A new hybrid method for solving SP flooding problems, its salient features, and some numerical results.
- Effect of viscoelasticity on the Saffman-Taylor instability (Ongoing)!
- Numerical studies with non-Newtonian models of SP flooding (Ongoing)!

Single- versus Multi-layer interfacial instability

Interaction between interfacial instabilities in EOR

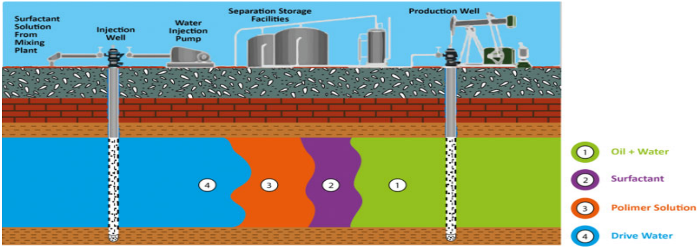

- A trailing interface can break through the leading interface long before the leading interface breaks through the production well.

Interaction between interfacial instabilities in EOR

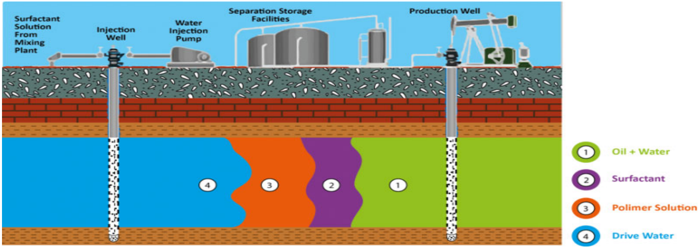

- A trailing interface can break through the leading interface long before the leading interface breaks through the production well.
- An interface in the presence of one or more interfaces in the multi-layer setting can be more unstable than what it would individually in the absence of other interfaces.

2-layer versus 3-layer interfacial instability in a HS cell

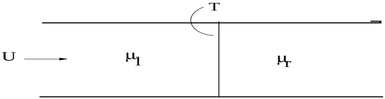

$$\sigma_{\max} = \frac{2T}{\mu_r + \mu_l}\left(\frac{U(\mu_r - \mu_l)}{3T}\right)^{3/2}$$

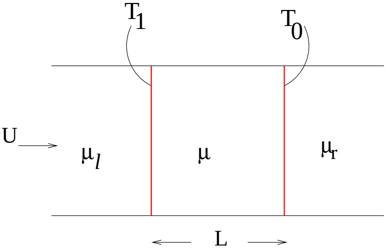

P. Daripa, "Hydrodynamic Stability of Multi-Layer Hele-Shaw Flows", *J. Stat. Mech.*, Article No. P12005, 2008.

$$\sigma < \sigma_{\mathrm{u}} = \max\left\{\frac{2T_0}{\mu_r}\left(\frac{U(\mu_r - \mu)}{3T_0}\right)^{3/2},\ \frac{2T_1}{\mu_l}\left(\frac{U(\mu - \mu_l)}{3T_1}\right)^{3/2}\right\}$$

$$\left(\frac{T_0}{T}\right)^{1/3} + \left(\frac{\mu_l}{\mu_r}\right)^{2/3}\left(\frac{T_1}{T}\right)^{1/3} > \left(1 + \frac{\mu_l}{\mu_r}\right)^{2/3}.$$

Multi-Layer Radial Flow (With Craig Gin)

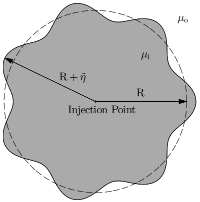

$$\sigma = \frac{\frac{Qn}{2\pi R^2}(\mu_o - \mu_i) - \frac{Tn(n^2-1)}{R^3}}{\mu_o + \mu_i} - \frac{Q}{2\pi R^2}$$

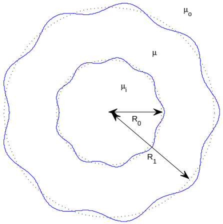

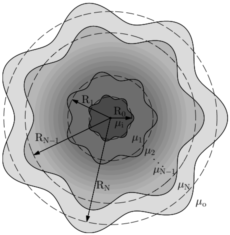

Next talk by **Craig Gin** will discuss this case in radial geometry.

Model of Chemical EOR (with Sourav Dutta)

SP Flood with Capillary Pressure and Dispersion

$$
\begin{aligned}
&-\nabla\cdot\left(\mathbf{K}(\mathbf{x})\lambda\nabla p_a\right)-\nabla\cdot\left(\mathbf{K}(\mathbf{x})\lambda_o\nabla p_c\right)=q_a+q_o,\\
&\frac{\partial\mathbf{U}}{\partial t}+\nabla\cdot\mathbf{F}(\mathbf{U})=\mathbf{Q}+\nabla\cdot\mathbf{G},
\end{aligned}
$$

where $p_c = p_o - p_a$, $\quad \mathbf{v}_i = -\mathbf{K}\lambda_i\nabla p_i\,(i=a,o)$, $\quad \mathbf{v}=\mathbf{v}_a+\mathbf{v}_o$.

$$
\mathbf{U}=\begin{pmatrix} s\\ c\,s\\ \Gamma\,s\end{pmatrix},\ \mathbf{F}=\begin{pmatrix} f_a\mathbf{v}\\ c\,f_a\mathbf{v}\\ \Gamma\,f_a\mathbf{v}\end{pmatrix},\ \mathbf{G}=\begin{pmatrix} 0\\ \mathbf{D}_c\nabla c\\ \mathbf{D}_\Gamma\nabla\Gamma\end{pmatrix},\ \mathbf{Q}=\begin{pmatrix} q_a\\ c^i q_a\delta(\mathbf{x}-\mathbf{x}^i)\\ \Gamma^i q_a\delta(\mathbf{x}-\mathbf{x}^i)\end{pmatrix}
$$

$\mathbf{C}=\mathbf{K}(\mathbf{x})f_a(s,c,\Gamma)\lambda_o(s,\Gamma)$, $\quad \mathbf{v}=\mathbf{v}_a+\mathbf{v}_o$ is the total velocity,
$p_c=p_c(s,\Gamma)$
$f_i(s,c,\Gamma)=\lambda_i(s,c,\Gamma)/\lambda(s,c,\Gamma)$,
$\lambda_i(s,c,\Gamma)=k_{ri}(s,\Gamma)/\mu_i(c)$, $\quad \lambda(s,c,\Gamma)=\lambda_a(s,c,\Gamma)+\lambda_o(s,c,\Gamma)$.
$\mathbf{D}_i(\mathbf{v})=d_{m,i}\mathbf{I}+|\mathbf{v}|(\mathbf{D}_{L,i}\mathbf{v}\mathbf{v}^T|\mathbf{v}|^{-2}+\mathbf{D}_{T,i}(\mathbf{I}-\mathbf{v}\mathbf{v}^T|\mathbf{v}|^{-2}))$, $(i=c,\Gamma)$.

Reformulation of the elliptic equation

$$-\nabla \cdot (\mathbf{K}(\mathbf{x})\lambda(s,c,\Gamma)\nabla p) = q_a + q_o.$$

Extended Chavent's global pressure formulation to incompressible two-component two-phase flows.

$$p = \frac{1}{2}(p_o + p_a) + \frac{1}{2}\int_{s_c}^{s} \chi(\zeta,c,\Gamma)\frac{dp_c}{d\zeta}(\zeta,\Gamma)\,d\zeta + \frac{1}{2}\int_{\Gamma_c}^{\Gamma} \chi(s,c,\xi)\frac{dp_c}{d\xi}(s,\xi)\,d\xi$$
$$-\frac{1}{2}\int \eta^c(s,c,\Gamma)\,dc - \frac{1}{2}\int \eta^s(s,c,\Gamma)\,ds - \frac{1}{2}\int \eta^\Gamma(s,c,\Gamma)\,d\Gamma + C$$

where $\chi(s,c,\Gamma) = \left(f_o - f_a\right)(s,c,\Gamma)$.

∘ G. Chavent and J. Jaffré , Mathematicals Models and Finite Elements for Reservoir Simulation, Amsterdam, North-Holland, 1986

∘ P. Daripa and S. Dutta, Modeling and simulation of surfactant polymer flooding using a new hybrid method, J. Comput. Phys. 335 (2017) 249-282.

Reformulated system of model equations for SP Flood

$$-\nabla\cdot(\mathbf{K}(\mathbf{x})\lambda(s,c,\Gamma)\nabla p) = q_a + q_o,$$
$$\frac{\partial \mathbf{U}}{\partial t} + \nabla\cdot\mathbf{F}(\mathbf{U}) = \mathbf{Q} + \nabla\cdot(\mathbf{G}-\mathbf{H}),$$

where $p_c = p_o - p_a$, $\quad \mathbf{v}_i = -\mathbf{K}\lambda_i\nabla p_i \, (i = a, o)$, $\quad \mathbf{v} = \mathbf{v}_a + \mathbf{v}_o$.

$$\mathbf{U} = \begin{pmatrix} s \\ c\,s \\ \Gamma\,s \end{pmatrix}, \mathbf{F} = \begin{pmatrix} f_a\mathbf{v} \\ c\,f_a\mathbf{v} \\ \Gamma\,f_a\mathbf{v} \end{pmatrix}, \mathbf{G} = \begin{pmatrix} 0 \\ \mathbf{D}_c\nabla c \\ \mathbf{D}_\Gamma\nabla\Gamma \end{pmatrix}, \mathbf{H} = \begin{pmatrix} \mathbf{C}\,\nabla p_c \\ c\,\mathbf{C}\,\nabla p_c \\ \Gamma\,\mathbf{C}\,\nabla p_c \end{pmatrix}, \mathbf{Q} = \begin{pmatrix} q_a \\ c^i q_a\delta(\mathbf{x}-\mathbf{x}^i) \\ \Gamma^i q_a\delta(\mathbf{x}-\mathbf{x}^i) \end{pmatrix}$$

$\mathbf{C} = \mathbf{K}(\mathbf{x})f_a(s,c,\Gamma)\lambda_o(s,\Gamma)$, $\quad \mathbf{v} = \mathbf{v}_a + \mathbf{v}_o$ is the total velocity,
$p_c = p_c(s,\Gamma)$
$f_i(s,c,\Gamma) = \lambda_i(s,c,\Gamma)/\lambda(s,c,\Gamma)$,
$\lambda_i(s,c,\Gamma) = k_{ri}(s,\Gamma)/\mu_i(c)$, $\quad \lambda(s,c,\Gamma) = \lambda_a(s,c,\Gamma) + \lambda_o(s,c,\Gamma)$.
$\mathbf{D}_i(\mathbf{v}) = d_{m,i}\mathbf{I} + |\mathbf{v}|(\mathbf{D}_{L,i}\mathbf{v}\mathbf{v}^T|\mathbf{v}|^{-2} + \mathbf{D}_{T,i}(\mathbf{I}-\mathbf{v}\mathbf{v}^T|\mathbf{v}|^{-2}))$, $(i = c, \Gamma)$.

DFEM-MMOC Hybrid Method

DFEM-MMOC based Hybrid Method

$$-\nabla \cdot (\mathbf{K}(\mathbf{x})\lambda(s,c,\Gamma)\nabla p) = q_a + q_o.$$

$$\frac{\partial \mathbf{U}}{\partial t} + \nabla \cdot \mathbf{F}(\mathbf{U}) = \mathbf{Q} + \nabla \cdot (\mathbf{G} - \mathbf{H}).$$

Step 1: Pressure equation

$$-\nabla \cdot (\mathbf{K}(\mathbf{x})\lambda(s,c,\Gamma)\nabla p) = q_a + q_o,$$

This is solved by a **Discontinuous Finite Element Method (DFEM)**.

Step 2: System of Transport equations: solved by **MMOC**

$$\phi\frac{\partial s}{\partial t} + \frac{\partial f_a}{\partial s}\mathbf{v}\cdot\nabla s + \nabla\cdot\left(\mathbf{C}\frac{\partial p_c}{\partial s}\nabla s\right) = g_s - \frac{\partial f_a}{\partial c}\mathbf{v}\cdot\nabla c - \frac{\partial f_a}{\partial \Gamma}\mathbf{v}\cdot\nabla\Gamma - \nabla\cdot\left(\mathbf{C}\frac{\partial p_c}{\partial \Gamma}\nabla\Gamma\right)$$

$$\phi\frac{\partial c}{\partial t} + \left(\frac{f_a}{s}\mathbf{v} + \frac{\mathbf{C}}{s}\left(\frac{\partial p_c}{\partial s}\nabla s + \frac{\partial p_c}{\partial \Gamma}\nabla\Gamma\right)\right)\cdot\nabla c - \frac{\phi}{s}\nabla\cdot(\mathbf{D}_c\cdot\nabla c) = g_c$$

$$\phi\frac{\partial \Gamma}{\partial t} + \left(\frac{f_a}{s}\mathbf{v} + \frac{\mathbf{C}}{s}\left(\frac{\partial p_c}{\partial s}\nabla s + \frac{\partial p_c}{\partial \Gamma}\nabla\Gamma\right)\right)\cdot\nabla\Gamma - \frac{\phi}{s}\nabla\cdot(\mathbf{D}_\Gamma\cdot\nabla\Gamma) = g_\Gamma$$

$\mathbf{C} = \mathbf{K}(\mathbf{x})f_a(s,c,\Gamma)\lambda_o(s,\Gamma)$, $\quad\mathbf{v} = \mathbf{v}_a + \mathbf{v}_o$ is the total velocity,
$f_i(s,c,\Gamma) = \lambda_i(s,c,\Gamma)/\lambda(s,c,\Gamma)$, $\quad p_c = p_c(s,\Gamma)$.
$\lambda_i(s,c,\Gamma) = k_{ri}(s,\Gamma)/\mu_i(c)$, $\quad\lambda(s,c,\Gamma) = \lambda_a(s,c,\Gamma) + \lambda_o(s,c,\Gamma)$.
$\mathbf{D}_i(\mathbf{v}) = d_{m,i}\mathbf{I} + |\mathbf{v}|(\mathbf{D}_{L,i}\mathbf{v}\mathbf{v}^T|\mathbf{v}|^{-2} + \mathbf{D}_{T,i}(\mathbf{I} - \mathbf{v}\mathbf{v}^T|\mathbf{v}|^{-2}))$, $(i = c,\Gamma)$.

Discontinuous Finite Element Method

$$-\frac{1}{N_c}\nabla\cdot\left(\mathbf{K}(\mathbf{x})\mu_o\lambda(s,c,\Gamma)\nabla p\right) = q_a + q_o, \quad \mathbf{x}\in\Omega\backslash\Sigma,$$

$$\left(\mathbf{K}(\mathbf{x})\lambda(s,c,\Gamma)\nabla p\right)\cdot\hat{\mathbf{n}} = 0, \quad \mathbf{x}\in\partial\Omega,$$

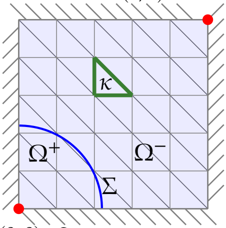

The weak formulation for the elliptic equation is written in the usual Sobolev spaces $H^1(\Omega)$ with $\psi\in H^1(\Omega)$ as:

$$\int_{\Omega^+}\mathbf{K}\lambda\nabla p\nabla\psi + \int_{\Omega^-}\mathbf{K}\lambda\nabla p\nabla\psi - \int_{\partial\Omega}\mathbf{K}\lambda\psi\nabla p.\hat{\mathbf{n}} = N_c\int_{\Omega}\tilde{q}\psi$$

where $\nabla p\cdot\hat{\mathbf{n}} = 0$ on $\partial\Omega$, $\tilde{q} = q_a + q_o$ and $[K(x)\lambda\nabla p\cdot\hat{\mathbf{n}}]_\Sigma = 0$.

The jumps in saturations at interfaces are incorporated in the finite element basis function in this method.

- P. Daripa, S. Dutta, J. Comput. Phys. 335 (2017), 249-282.
- S. Hou, W. Wang, L. Wang, J. Comput. Phys. 229 (2010) 7162-7179.

Modified Method of Characteristics

Reformulation of the Transport Equations:

$$\psi_s \frac{\partial s}{\partial \tau_s} + \nabla\cdot\left(\mathbf{C}\frac{\partial p_c}{\partial s}\nabla s\right) = g_s - \frac{\partial f_a}{\partial c}\mathbf{v}\cdot\nabla c - \frac{\partial f_a}{\partial \Gamma}\mathbf{v}\cdot\nabla\Gamma - \nabla\cdot\left(\mathbf{C}\frac{\partial p_c}{\partial \Gamma}\nabla\Gamma\right),$$

$$\psi_c \frac{\partial c}{\partial \tau_c} - \frac{\phi}{s}\nabla\cdot(\mathbf{D}_c\cdot\nabla c) + cg = g_c,$$

$$\psi_\Gamma \frac{\partial \Gamma}{\partial \tau_\Gamma} - \frac{\phi}{s}\nabla\cdot(\mathbf{D}_\Gamma\cdot\nabla\Gamma) + \Gamma g = g_\Gamma.$$

where $g_s = (1-f_a)Q\delta(\mathbf{x}-\mathbf{x}^i)$, $g_c = \frac{c^iQ}{s}\delta(\mathbf{x}-\mathbf{x}^i)$, $g_\Gamma = \frac{\Gamma^iQ}{s}\delta(\mathbf{x}-\mathbf{x}^i)$, and $g = \frac{Q}{s}\delta(\mathbf{x}-\mathbf{x}^i)$ are the point source terms with δ being the Dirac delta function.

Numerical Method: Finite Difference MMOC

Flowchart

Governing equations:

$$
\begin{aligned}
&-\nabla \cdot \left(\mathbf{K}\lambda \nabla p\right) = \tilde{q},\\
&\psi_s \frac{\partial s}{\partial \tau_s} + \nabla \cdot \left(\mathbf{C}\frac{\partial p_c}{\partial s}\nabla s\right) = g_s - \frac{\partial f_a}{\partial c}\mathbf{v}\cdot\nabla c - \frac{\partial f_a}{\partial \Gamma}\mathbf{v}\cdot\nabla\Gamma - \nabla\cdot\left(\mathbf{C}\frac{\partial p_c}{\partial \Gamma}\nabla\Gamma\right),\\
&\psi_c \frac{\partial c}{\partial \tau_c} - \frac{\phi}{s}\nabla\cdot\left(\mathbf{D}_c \cdot \nabla c\right) + cg = g_c,\\
&\psi_\Gamma \frac{\partial \Gamma}{\partial \tau_\Gamma} - \frac{\phi}{s}\nabla\cdot\left(\mathbf{D}_\Gamma \cdot \nabla \Gamma\right) + \Gamma g = g_\Gamma.
\end{aligned}
$$

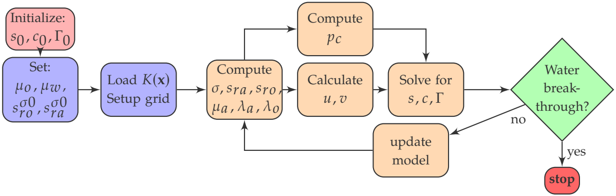

Comparison Floods: Rectilinear Geometry

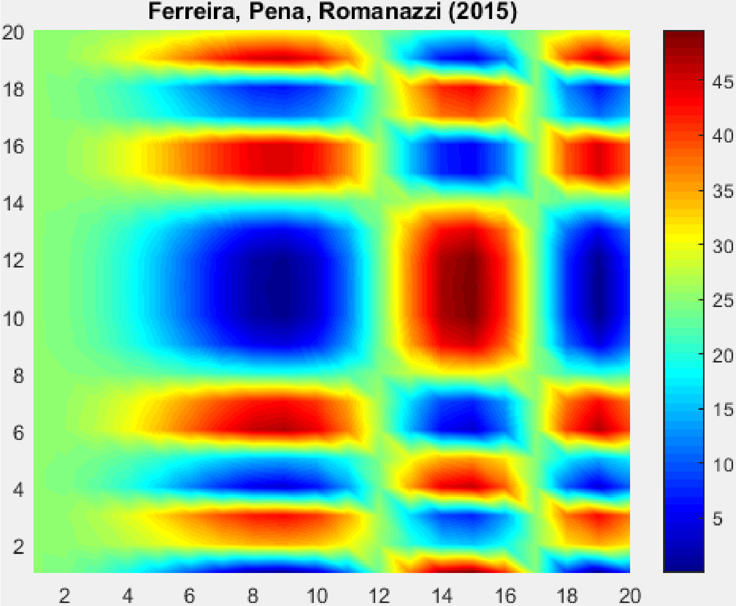

Comparison Floods: Quarter Five-Spot

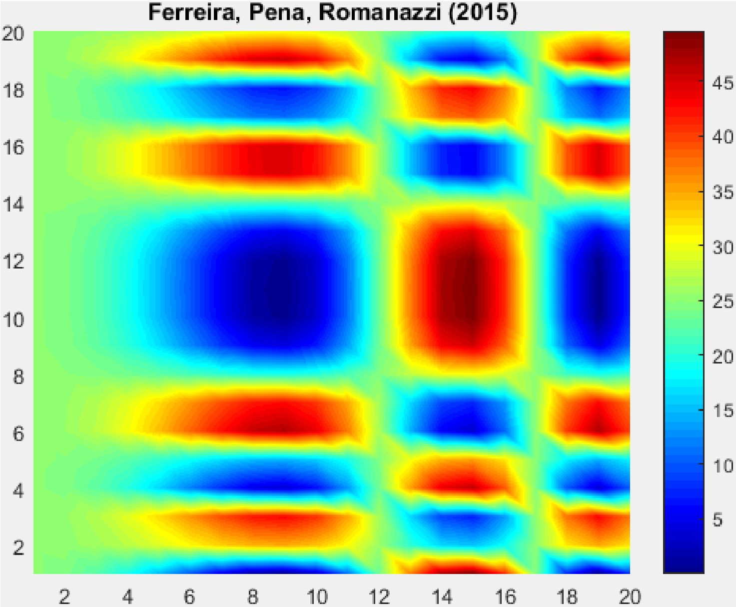

Viscoelastic Effects

Towards Viscoelastic Fingering in a Hele-Shaw Cell

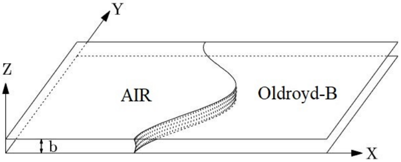

- Continuity equation and Flow equations.

$$\nabla \cdot \mathbf{v} = 0, \quad -\nabla p + \nabla \cdot \tau = \mathbf{0}.$$

- Constitutive relation: $\tau + \lambda_1 \tau^{\nabla} = \mu[D + \lambda_2 D^{\nabla}]$
  λ_1, λ_2: relaxation and retardation (time) constants. τ^{∇} and D^{∇} are given by

$$\tau^{\nabla} = \tau_t + \mathbf{v} \cdot \nabla \tau - (L\tau + \tau L^T),$$

$$D^{\nabla} = D_t + \mathbf{v} \cdot \nabla D - (LD + DL^T).$$

where $L = \nabla \mathbf{v}, \quad D = L + L^T$.

Dispersion Relation

- Averaging of **the Laplace law** across the plates.

$$\sigma = \frac{\left[< u^0 > (1 - Ca^{-1})\, k - \left(\frac{b^2}{12}\right)\ \frac{\gamma}{\mu} k^3 \right]}{1 - 4 < u^0 > (\lambda_1 - \lambda_2)k + b^2k^2/6},$$

where $Ca = < u^0 > \mu/\gamma$ is the Capillary number.

- Notice that this formula for the growth rate is of the form

$$\sigma(k) = \frac{a_1\, k - a_2\, k^3}{1 - \beta k + a_3 k^2},$$

where β is a multiple of the elasticity measure $\lambda_1 - \lambda_2$ and a_1, a_2, a_3 are constants.

Plot of the Dispersion Relation

$$\sigma(k) = \frac{k - 0.5k^3}{1 - \beta k + k^2}.$$

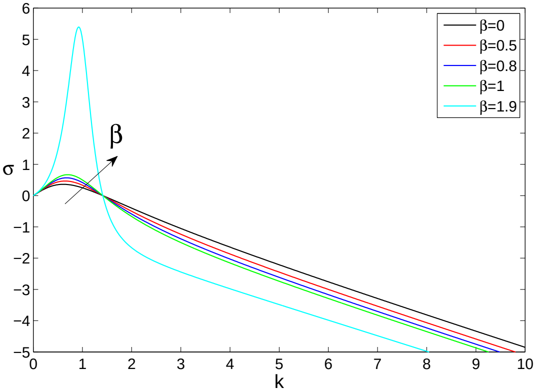

Figure: Plot of growth rate σ versus k for several values of $\beta = 4 < u^0 > (\lambda_1 - \lambda_2)$. Collaborator: Gelu Pasa

Previous Results

Relaxation time constants: $\lambda_1, \lambda_2, \quad \lambda_1 > \lambda_2$.

Weissenberg number: W_1 is proportional to λ_1

From Wilson(1990, JFM): Numerical results show that elasticity is destabilizing for Saffman-Taylor instability.

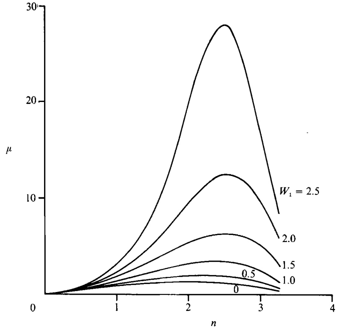

Reservoir Scale Modeling of Viscoelastic Effects - Ongoing

Two-phase, two-component, non-Newtonian model

$$
\begin{aligned}
\mathbf{v}_a &= \mathbf{K}(\mathbf{x})\lambda_a(We^2|\nabla p_a|^2)(-\nabla p_a + \rho_a \mathbf{g}),\\
\mathbf{v}_o &= \mathbf{K}(\mathbf{x})\lambda_o(We^2|\nabla p_o|^2)(-\nabla p_o + \rho_o \mathbf{g}),\\
p_o - p_a &= p_c(s,\Gamma),\\
\nabla\cdot(\mathbf{v}_a + \mathbf{v}_o) &= \frac{q_a}{\rho_a} + \frac{q_o}{\rho_o}\\
\phi\frac{\partial s}{\partial t} + \nabla\cdot(\mathbf{v}_a) &= \frac{q_a}{\rho_a},\\
\phi\frac{\partial (sc)}{\partial t} + \nabla\cdot(c\mathbf{v}_a) &= c_{inj}\frac{q_a}{\rho_a},\\
\phi\frac{\partial (s\Gamma)}{\partial t} + \nabla\cdot(\Gamma\mathbf{v}_a) &= \Gamma_{inj}\frac{q_a}{\rho_a}.
\end{aligned}
$$

.

Conclusion

Summary

- We have shown only one upper bound result on the growth rate of viscosity driven instability in thre-layer rectilinear Hele-Shaw flows in order to explain the significance of such multi-layer stability studies to enhanced oil recovery processes. Many more results on stability of such flows can be found in my publications with co-authors. Talks by Craig Gin and Zhiying Hai in this minisymposium will showcase some of such results.

Summary

- We have shown only one upper bound result on the growth rate of viscosity driven instability in thre-layer rectilinear Hele-Shaw flows in order to explain the significance of such multi-layer stability studies to enhanced oil recovery processes. Many more results on stability of such flows can be found in my publications with co-authors. Talks by Craig Gin and Zhiying Hai in this minisymposium will showcase some of such results.
- We have presented a numerical method to solve a system of elliptic and transport equations. This method uses a discontinuous finite element method (DFEM) to solve the elliptic equation and a modified method of characteristics (MMOC).

Summary

- We have shown only one upper bound result on the growth rate of viscosity driven instability in thre-layer rectilinear Hele-Shaw flows in order to explain the significance of such multi-layer stability studies to enhanced oil recovery processes. Many more results on stability of such flows can be found in my publications with co-authors. Talks by Craig Gin and Zhiying Hai in this minisymposium will showcase some of such results.
- We have presented a numerical method to solve a system of elliptic and transport equations. This method uses a discontinuous finite element method (DFEM) to solve the elliptic equation and a modified method of characteristics (MMOC).
- We have extended the Chavent's definition of global pressure from two-phase porous media flows to two-phase **two-component** porous media flows.

Summary Continued:

- We have presented numerical solutions of realistic chemical EOR problems.

Summary Continued:

- We have presented numerical solutions of realistic chemical EOR problems.
- We have presented results, in particular growth rate formula which shows catastrophic growth rate for Weisenberg number in certain range.

Summary Continued:

- We have presented numerical solutions of realistic chemical EOR problems.
- We have presented results, in particular growth rate formula which shows catastrophic growth rate for Weisenberg number in certain range.
- Currently the work is ongoing in incorpoating viscoelastic effects in our model and simulation.

Some references

P. Daripa,
Hydrodynamic Stability of Multi-Layer Hele-Shaw Flows. *J. Stat. Mech.*, Article No. P12005, 2008. Doi: 10.1088/1742-5468/2009/07/L07002

P. Daripa and S. Dutta,
Modeling and simulation of surfactant-polymer flooding using a new hybrid method. *J. Comput. Phys.*, 335:249-282, 2017.

P. Daripa and S. Dutta,
Convergence analysis of a characteristics-based hybrid method for multicomponent transport in porous media. *arXiv:1707.00035*, 2017.

C. Gin and P. Daripa,
Stability Results for Multi-Layer Radial Hele-Shaw and Porous Media Flows. *Physics of Fluids*, 27, 012101 2014. doi: 10.1063/1.4904983

G. Chavent and J. Jaffré,
Mathematical Models and Finite Elements for Reservoir Simulation. *Elsevier Science Ltd.* Amsterdam, North-Holland, 1986.

Jim Douglas Jr.
Finite Difference Methods for Two-Phase Incompressible Flow in Porous Media. *SIAM Journal on Numerical Analysis*, 20:681-696, 1983.

Songming Hou, Wei Wang, Liqun Wang
Numerical method for solving matrix coefficient elliptic equation with sharp-edged interfaces. *Journal of Comp. Phy.*, 229:7162-7179, 2010.

Acknowledgment

This talk has been made possible by the NPRP grant No. 08-777-1-141 through Qatar National Research Fund and by the U.S. National Science Foundation Grant No. DMS 1522782.

THE END

Thank you.

Questions?

Appendix

EXTRA SLIDES

Constitutive Relations

Linear Viscosity model:

$$\mu_a = \mu_w(1 + \beta c) \tag{1}$$

Here β is a constant dependent on the types of polymer and rock.
μ_w = viscosity of pure water.

Capillary pressure: p_c (Brown and Pope, 1994)

$$p_c = \left(\sigma\omega_2\sqrt{\phi/K}\right)\left(1 - \frac{s - s_{ra}^{\sigma}}{1 - s_{ra}^{\sigma} - s_{ro}^{\sigma}}\right)^{-1/\omega_1} \tag{2}$$

where $\sigma = \sigma(\Gamma)$ is the interfacial tension, ω_1 is the pore-size index, $s_{ri}^{\sigma}\,(i = a, o)$ are the phase residual saturations when the interfacial tension is $\sigma = \sigma(\Gamma)$.

Relative Permeabilities:

When $\Gamma = 0$ (Brooks and Corey, 1966)

$$
\begin{aligned}
k_{ra}^{\sigma 0} &= \left(\frac{s - s_{ra}^{\sigma 0}}{1 - s_{ra}^{\sigma 0}}\right)^{\frac{2+3\theta}{\theta}}, \\
k_{ro}^{\sigma 0} &= \left(1 - \frac{s - s_{ra}^{\sigma 0}}{1 - s_{ra}^{\sigma 0} - s_{ro}^{\sigma 0}}\right)^2 \left[1 - \left(\frac{s - s_{ra}^{\sigma 0}}{1 - s_{ra}^{\sigma 0} - s_{ro}^{\sigma 0}}\right)^{\frac{2+\theta}{\theta}}\right],
\end{aligned}
\tag{3}
$$

where the parameter $\theta = 2$ in our simulations.

When $\Gamma \neq 0$ (Amaefule and Handy, 1982)

$$
\begin{aligned}
k_{ra}^{\sigma} &= \left(\frac{s - s_{ra}^{\sigma}}{1 - s_{ra}^{\sigma}}\right) \left\{2.5 s_{ra}^{\sigma} \left[\left(\frac{s - s_{ra}^{\sigma}}{1 - s_{ra}^{\sigma}}\right)^2 - 1\right] + 1\right\}, \\
k_{ro}^{\sigma} &= \left(1 - \frac{s - s_{ra}^{\sigma}}{1 - s_{ra}^{\sigma} - s_{ro}^{\sigma}}\right) \left\{5 s_{ro}^{\sigma} \left[\left(1 - \frac{s - s_{ra}^{\sigma}}{1 - s_{ra}^{\sigma} - s_{ro}^{\sigma}}\right) - 1\right] + 1\right\}.
\end{aligned}
\tag{4}
$$

Constitutive Relations

Residual Saturations: (Amaefule and Handy, 1982)

$$s_{ro}^{\sigma} = \begin{cases} s_{ro}^{\sigma 0} & N_c < N_{co} \\ s_{ro}^{\sigma 0}\left(\frac{N_{co}}{N_c}\right)^{0.5213} & N_c \geq N_{co} \end{cases}, \tag{5}$$

$$s_{ra}^{\sigma} = \begin{cases} s_{ra}^{\sigma 0} & N_c < N_{cao} \\ s_{ra}^{\sigma 0}\left(\frac{N_{cao}}{N_c}\right)^{0.1534} & N_c \geq N_{cao} \end{cases}. \tag{6}$$

where $N_c = \frac{|\mathbf{v}|\mu}{\sigma}$ is the **capillary number** of the aqueous phase, N_{co} and N_{cao} are the **critical capillary numbers** of the oil and the aqueous phase respectively.

Interfacial tension: (Liu *et al.* , 2007)

$$\sigma = \frac{10.001}{\Gamma + 1} - 0.001 \tag{7}$$

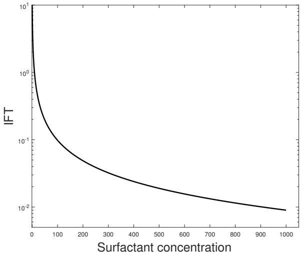

Figure: Interfacial tension(IFT) of oil/brine as a function of Γ

Grid Orientation effect

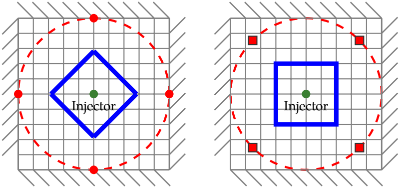

(a) Parallel (b) Diagonal

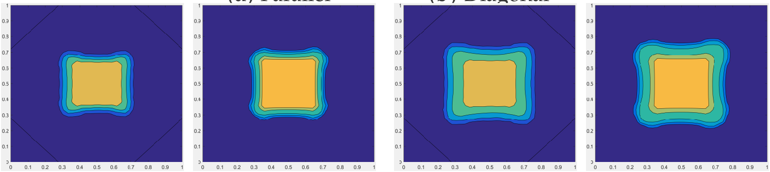

(c) $t = 200$, parallel flood (d) $t = 200$, diagonal flood (e) $t = 400$, parallel flood (f) $t = 400$, diagonal flood

Figure: Comparison of water saturation contours for parallel and diagonal flow simulations in a five-spot geometry with a spatial resolution of 40×40 to study the grid orientation effects at **viscosity ratio** $M_\mu = 20$. Subfigures (c) and (e) correspond to parallel flows while (d) and (f) correspond to the diagonal flow simulations at two different time levels, $t = 200$ and $t = 400$.

Input Data

Domain & Input parameters:

$\Omega = [0,1]^2$ and absolute permeability, $\mathbf{K} = 1$.

Table: Simulation input data

Model parameter	Symbol	Value
Spatial grid size	$h \times k$	variable
Porosity	ϕ	1
Permeability	$\mathbf{K}$	variable
Initial resident water saturation	$s_0^{\sigma 0}$	0.21
Polymer injection concentration	c_0	variable
Surfactant injection concentration	Γ_0	variable
Oil viscosity	μ_o	12.6
Pure water viscosity	μ_w	1.26
Residual aqueous phase saturation	s_{ra}	0.1
Residual oleic phase saturation	s_{ro}	0.2
Critical capillary number of aqueous phase	N_{cao}	10^{-5}
Critical capillary number of oleic phase	N_{co}	10^{-5}
Parameters of capillary pressure relation	ω_1, ω_2	$0.1, 0.4$
Injection rate	Q	$200, 50$
Time step size	Δt	$1/25, 1/100$